

AD-787 487

CONDUCTION MECHANISMS IN THICK FILM  
MICROCIRCUITS

R. W. Vest

Purdue Research Foundation  
Lafayette, Indiana

1 August 1974

DISTRIBUTED BY:

**NTIS**

National Technical Information Service  
U. S. DEPARTMENT OF COMMERCE  
5285 Port Royal Road, Springfield Va. 22151

AD 787 487

Semi-Annual Technical Report  
for the Period 1/1/74-6/30/74

CONDUCTION MECHANISMS IN THICK FILM MICROCIRCUITS

Grant Number: DAHC15-73-G8

ARPA Order No.: 1001/192

Grantee: Purdue Research Foundation

Principal Investigator: R. W. Vest  
(317) 749-2601

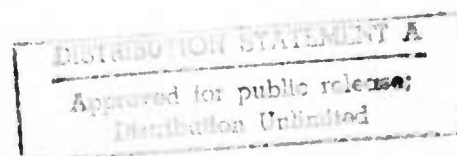
Effective Date of Grant: 7/1/73

Grant Expiration Date: 6/30/75

Amount of Grant: \$77,923

Reproduced by  
NATIONAL TECHNICAL  
INFORMATION SERVICE  
U S Department of Commerce  
Springfield VA 22151

August 1, 1974



## Forward

Research described in this report constitutes the eighth six months effort under two grants from the Defense Advance Research Projects Agency, Department of Defense, under the technical cognizance of Dr. Norman Tallan, Aerospace Research Laboratories, U. S. Air Force. Copies of previous reports are available from Defense Documentation Center, Cameron Station, Alexandria, VA., 22314. The research was conducted in the Turner Laboratory for Electroceramics, School of Electrical Engineering and School of Materials Engineering, Purdue University, West Lafayette, Indiana 47907, under the direction of Professor R. W. Vest. Contributing to the project were Assistant Professor G. L. Fuller, Messrs. D. J. Deputy, A. N. Prabhu, and R. L. Reed. The level of effort was drastically reduced, beginning January 1, 1974, so that sufficient funds would be available for two graduate students to complete their thesis research under the one year, no cost, time extension granted by ARPA.

## ABSTRACT

It was demonstrated that neither direct observation of neck growth nor measurements of the shrinkage of composites can be applied to establish initial stage sintering kinetics for  $\text{RuO}_2$  in the presence of glass. Three secondary measurement techniques (microstructure determination, X-ray line broadening, and surface area measurements) were employed and results were shown to be consistent among the three techniques.

Studies of the ripening process whereby large crystals of  $\text{RuO}_2$  grow in the glassy matrix uncovered a strong chemical interaction between the glass and the alumina substrate which significantly influences the rate of the ripening process. In particular, the substrate tends to inhibit the growth of  $\text{RuO}_2$  crystals, which is a desirable situation if the conductive network is to be preserved.

## TABLE OF CONTENTS

	Page
I. Introduction .....	1
II. Microstructure Development.....	3
A. Experimental Techniques.....	3
B. Sample Preparation.....	5
C. Results and Discussion.....	7
III. Summary and Future Plans.....	24
IV. References.....	26
V. Distribution List.....	28

## LIST OF FIGURES

		<u>Page</u>
1	Microstructure of Shrinkage Samples (x 1000).	6
2	Sintering and Growth of RuO <sub>2</sub> Particles. Paste Fired in a Platinum Boat (Sample 3) 10,000 x.	9
3	Sintering and Growth of RuO <sub>2</sub> Particles. Powder Mixture Figure in a Platinum Crucible at 1000°C (Sample 4) 10,000.	10
4	Sintering and Growth of RuO <sub>2</sub> Particles. Powder Mixture Fired in a Platinum Crucible (Sample 4) 10,000 x.	11
5	Sintering With Limited Growth of RuO <sub>2</sub> Particles. Paste Fired on Al Si Mag 614 Substrates (Sample 1) 10,000 x.	12
6	Effect of the Substrate on Growth of RuO <sub>2</sub> Particles. 1000°C, 6 hours, 10,000 x.	14
7	Average Crystallite Size From X-Ray Line Broadening.	15
8	Particle Size of Sample 4 From X-Ray and Surface Area.	19
9	Surface Area of Sample 4.	21
10	Liquid Phase Sintering Geometry.	22
11	Sintering and Growth of RuO <sub>2</sub> Particles - 18 w/o RuO <sub>2</sub> Plus Glass Powder Mixture Fired in a Platinum Crucible at 1000°C (10,000 x).	24

## I. Introduction

Advances in thick film technology have been hindered by an inadequate understanding of the relationships between the physical properties of the ingredient materials and the electrical properties of the resulting resistors and conductors. The lack of a predictive model of the conduction mechanism has hampered the development of new materials, as well as the improvement of existing systems. The two primary concerns of the present research program in the area of resistor technology are the development of adequate models to describe the "Blending Curve Anomaly" and the "TCR Anomaly." The "Blending Curve Anomaly" refers to the often reported observation that with oxidic conductors and glass the sheet resistance varies monotonically from very low (e.g., 1 v/o) to very high conductive concentrations; whereas, with noble metal conductives and glass electrical continuity is not achieved until the amount of conductive approaches 30 v/o or higher. The primary scientific question is: what are the driving forces which are responsible for the formation of continuous conducting paths along the length of the resistor at such low concentrations of the conductive? The "TCR Anomaly" refers to the fact the temperature coefficient of resistance of a resistor is much lower than the TCR of any of the individual ingredients from which it was made. The primary scientific question is: what is the mechanism by which electric charge is transported?

The primary thrust of the experimental program is to relate electrical properties of the thick films to the materials properties and processing conditions through microstructure. The materials properties to be correlated

are: resistivity, temperature coefficient of resistivity, coefficient of thermal expansion, interfacial energy, particle shape, size and size distribution, and chemical reactivity with other constituents. The processing conditions to be correlated are time, temperature and atmosphere during firing. The specific objectives of the program are:

1. Determine the dominant sintering mechanisms responsible for microstructure development and establish the relative importance of the various properties of the ingredient materials.
2. Determine the dominant mechanisms limiting electrical charge transport, and establish the relative importance of the various properties of the ingredient materials.
3. Develop phenomenological models to interrelate the various materials properties with systems performance.

Earlier work in these three areas have been previously reported {1-7}.



## II. Microstructure Development

The electrical properties of a thick film resistor depend directly on the microstructure that is formed during the firing cycle, normally executed with a tunnel kiln. The proposed model of microstructural development (8) predicts a sequence of steps involving sintering of the glass; wetting the conductive particles, attraction of the conductive particles to form a continuous network, sintering of the conductive particles, and finally destruction of the conductive network. Studies described in this report were directed toward elucidating the last two steps.

### A. Experimental Techniques.

Previously reported (9) attempts to observe neck growth between two ground  $\text{RuO}_2$  crystals (size range 150-300  $\mu\text{m}$ ) heated at 800°C for 3 hours in the presence of the lead-borosilicate glass (63%  $\text{PbO}$  - 25%  $\text{B}_2\text{O}_3$  - 12%  $\text{SiO}_2$ ) failed to indicate any evidence of sintering. Further experiments were carried out with similar crystals but employing higher temperatures (up to 1000°C) and longer time duration (up to 100 hours). After the heat treatment the glass was completely leached out using successive  $\text{HCl}$  and  $\text{HF}$  treatments. This procedure has been previously demonstrated (10) to quantitatively remove the glass while leaving  $\text{RuO}_2$  completely unaffected. After all the glass was leached out, the  $\text{RuO}_2$  crystals were in their original form, indicating that no neck growth had occurred during heating. This result was undoubtedly due to the slow kinetics resulting from the large particle size. Still higher temperatures cannot be employed as the  $\text{RuO}_2$  loss becomes appreciable, and significantly smaller particles cannot be used because of limitations in the resolving power of the optical system of the hot stage

metallograph. Hot stage scanning electron microscopy or transmission electron microscopy cannot be easily adopted for the  $\text{RuO}_2$ -lead borosilicate glass system as the use of vacuum or any inert atmosphere reduces the glass and  $\text{RuO}_2$ . As a result of these considerations, alternate methods to determine the sintering kinetics were studied.

Measurements of density and dimension changes of compacts upon heating have the potential of providing information about the initial stages of liquid phase sintering. In order to study the feasibility of this approach, preliminary measurements were carried out to record the dimensional changes of compacts of  $\text{RuO}_2$  and glass powders after sintering. The sub-micron particle size  $\text{RuO}_2$  was prepared by drying the hydrate following the method previously described (11). The mixture of glass and  $\text{RuO}_2$  powders (40-80 v/o  $\text{RuO}_2$ ) was dispersed thoroughly in an agate ball mill and pressed in the form of cylindrical pellets in a uniaxial press or an isostatic press at pressures varying from 40,000 to 100,000 psi. The pellets were in general 1/2 cm. long and 1/2 cm. in diameter with green densities from 50 to 70% of theoretical. These pellets were placed in a platinum boat and fired in a tube furnace at temperatures ranging from 800°C to 1000°C. No appreciable dimensional changes occurred even after heating for as long as 50 hours at 1000°C. Microstructural investigation of the compacts after firing with the SEM (Fig. 1) revealed considerable closed porosity in the samples. As the firing time was increased, the pores increased in size, but the total pore volume did not decrease appreciably. Grinding and reheating gave increased density, but these data do not give any information regarding the initial stage sintering. The sintering cannot be carried out under vacuum as both the glass and  $\text{RuO}_2$  are not stable under these conditions.

Since neither neck growth nor shrinkage experiments proved practical, three secondary techniques were employed to obtain data which could be related to the liquid phase sintering and/or ripening of  $\text{RuO}_2$  in the presence of glass.

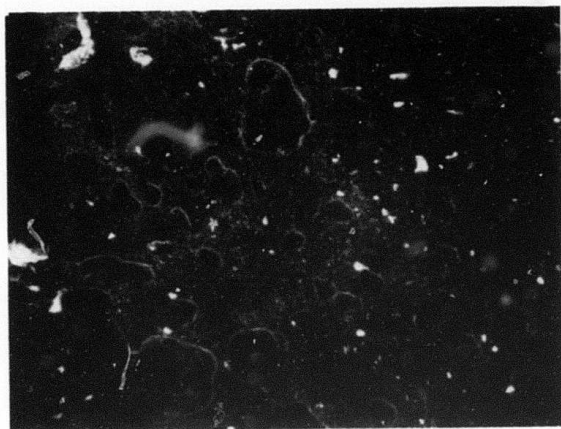
1. Microstructural development: As described in a previous report, (12) the final stage of sintering in the  $\text{RuO}_2$ -lead borosilicate glass system has been characterized as Ostwald ripening, where the small particles dissolve and precipitate on the larger ones, thus increasing their size. By following the mean particle size with time at any temperature, one can determine the kinetics of ripening process.

2. X-ray diffraction line broadening experiments can serve as a tool to study ripening kinetics, provided one is concerned with crystallite sizes below about  $0.2 \mu\text{m}$ .

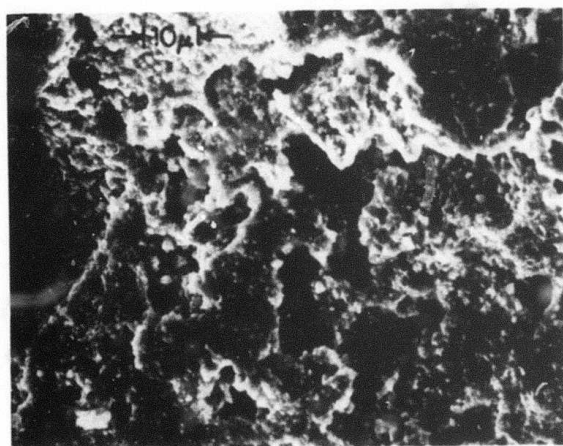
3. Surface Area Measurements: The network formation due to the particle-to-particle contacts, and the dissolution of smaller particles gives rise to a decrease in the surface area of the  $\text{RuO}_2$ . By measuring the surface area changes in  $\text{RuO}_2$  powder after the glass is removed it should be possible to follow the initial stage sintering.

#### B. Sample Preparation.

Samples were prepared from either a paste containing 40 w/o  $\text{RuO}_2$  relative to glass with ethyl cellulose-butyl carbitol screening agent, or a dry mixture of  $\text{RuO}_2$  and glass powder (18 or 30 w/o  $\text{RuO}_2$ ). The  $\text{RuO}_2$  in both the cases was made by drying the hydrate according to the procedure previously described (11). Whenever the paste was used, the samples were dried at  $125^\circ\text{C}$  and  $250^\circ\text{C}$  for half an hour before the final firing. The



a. Polished Surface (80%  $\text{RuO}_2$ , 800°C, 10 min.)



b. Fracture Surface (40%  $\text{RuO}_2$ , 1000°C, 2 hours)

Figure 1. Microstructure of Shrinkage Samples (x1000).

powders were thoroughly dispersed in the agate ball mill before use. The firing temperatures used were 800°C, 900°C, 1000°C, and 1100°C.

Samples were prepared in five different ways and will subsequently be referred to as sample types 1-5.

1. The paste screen printed in the form of square patterns (1 cm X 1 cm) on AlSiMag 614 substrates (96%  $\text{Al}_2\text{O}_3$ ).
2. The paste hand printed on platinum foil.
3. The paste fired in a platinum boat.
4. Mixture of  $\text{RuO}_2$  and glass powders heated in a platinum crucible.
5. Mixture of  $\text{RuO}_2$  and glass powders, along with pieces of AlSiMag 614 substrates, heated in a platinum crucible.

Since the aim was to look at the growth of  $\text{RuO}_2$  particles only, all the glass was completely leached out as described previously and only the  $\text{RuO}_2$  remaining was used for the analyses. Removal of all the glass was confirmed by energy dispersive X-ray analysis on the SEM, and by X-ray diffraction analysis on the Philips Norelco Diffractometer.

### C. Results and Discussion.

Figures 2 and 3 show the sintering and growth of  $\text{RuO}_2$  particles at 1000°C with increasing firing time for sample types 3 and 4 respectively. Figure 2a. shows the  $\text{RuO}_2$  powder after leaching out the glass but prior to any sintering or grain growth. Two features can be observed with increasing time at 1000°C in Figs. 2 and 3 for both sample types: a sintered network of  $\text{RuO}_2$  is formed with individual particles in the network maintaining approximately the same size as in the starting material; and large crystals of  $\text{RuO}_2$

begin to form with increasing time. The material for the formation of these crystals must come by partial dissolution of the sintered network. Figure 2d. shows that the sintered mat of  $\text{RuO}_2$  co-exists with the larger crystals after sufficient time at  $1000^\circ\text{C}$ . The two growth habits of the  $\text{RuO}_2$  crystals (platelets and needles) can also be easily seen in Fig. 2d. It can also be noted by comparing Figs. 2 and 3 that essentially identical crystal growth patterns are obtained, starting with a typical thick film paste or starting with only the mixture of the inorganic powders.

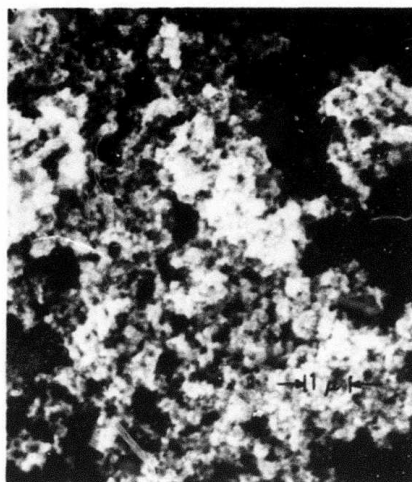
In addition to being a function of time at temperature, the sintering and growth are also functions of temperature. Figure 4 shows the microstructure obtained after two experiments using sample type 4 at  $800^\circ$  and  $900^\circ\text{C}$  firing temperatures. Even after 22-1/2 hours at  $800^\circ\text{C}$  there is almost no indication of particle growth; whereas, extensive particle growth is apparent after 6 hours at  $900^\circ\text{C}$ . These results raised hopes that we would be able to separate the sintering and growth phenomena and obtain quantitative kinetic data on both; however, results using sample type 1, which approximates an actual thick film resistor, did not agree with those obtained with sample types 3 or 4.

Figure 5 shows the microstructure obtained at  $900^\circ$ ,  $1000^\circ$  and  $1100^\circ\text{C}$  for differing times, and even at  $1100^\circ\text{C}$ , only very limited crystal growth can be detected. Figure 5b. can be compared with Figs. 2d. and 3d. which represent comparable time-temperature conditions for sample type 3 and 4. There is evidence of extensive sintering in Fig. 5b., but essentially no crystal growth.

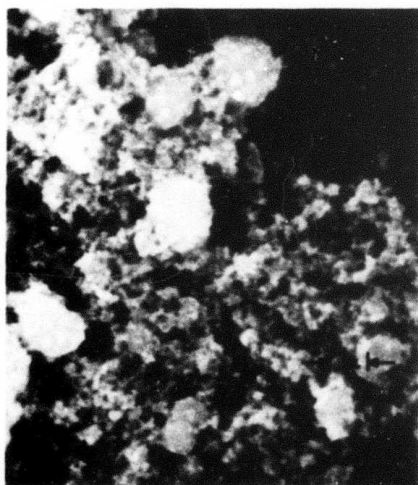
In order to separate possible effects due to geometry of the sample from those resulting from chemical interactions with the substrate, a sample was prepared by printing the paste on platinum foil (sample type 2), and the microstructure observed after 6 hours at  $1000^\circ\text{C}$  is shown in Fig. 6a. The



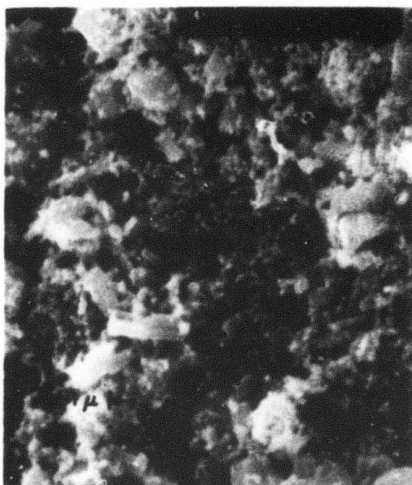
a. Dried at 250°C



b. 1000°C for 30 minutes



c. 1000°C for 2 hours

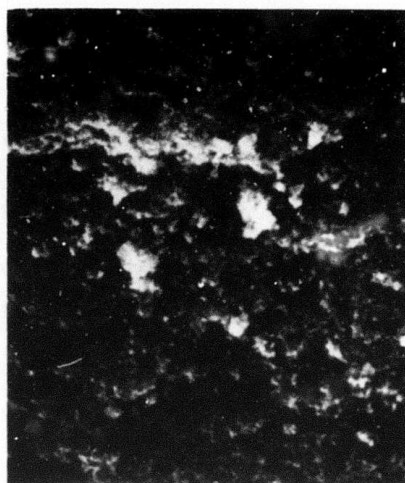


d. 1000°C for 6 hours

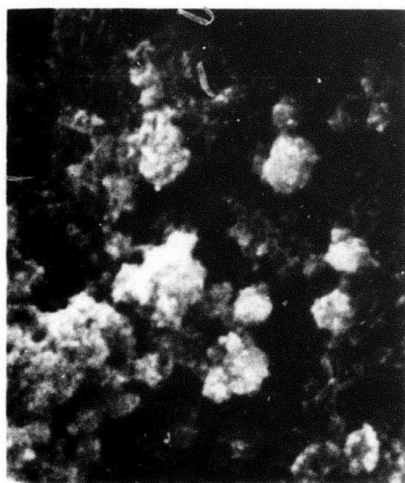
Figure 2. Sintering and Growth of  $\text{RuO}_2$  Particles. Paste Fired in a Platinum Boat (Sample 3) 10,000 x.



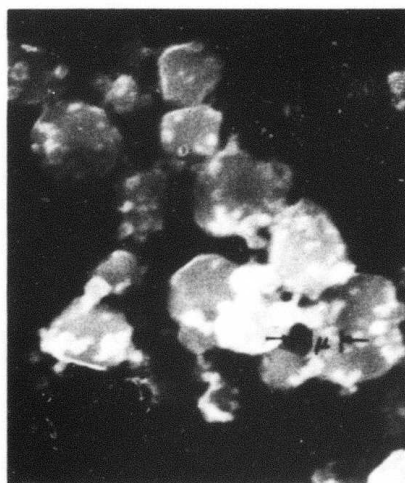
a. 5 minutes



b. 10 minutes



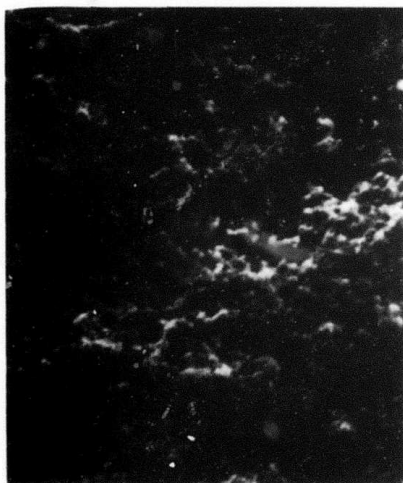
c. 30 minutes



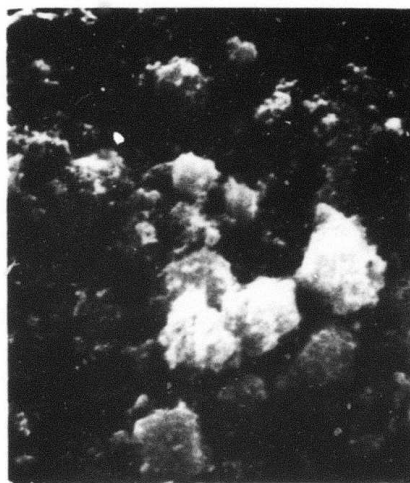
d. 6 hours

Figure 3. Sintering and Growth of  $\text{RuO}_2$  Particles. Powder Mixture Figure in a Platinum Crucible at  $1000^\circ\text{C}$  (Sample 4) 10,000.





a. 800°C, 22 1/2 hours

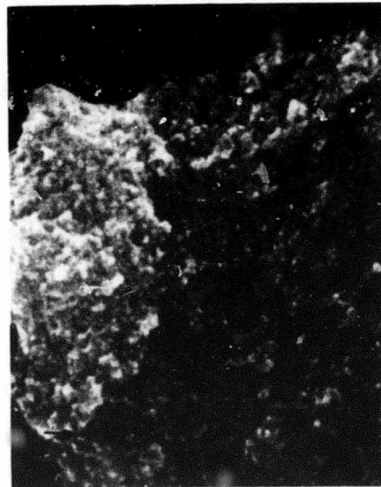


b. 900°C, 6 hours

Figure 4. Sintering and Growth of  $\text{RuO}_2$  Particles. Powder Mixture Fired in a Platinum Crucible(Sample 4) 10,000 x.



a. 900°C, 18 hours



b. 1000°C, 6 hours



c. 1100°C, 1.5 hours

Figure 5. Sintering with Limited Growth of  $\text{RuO}_2$  Particles. Paste Fired on Al Si Mag 614 Substrates (Sample 1) 10,000 x.

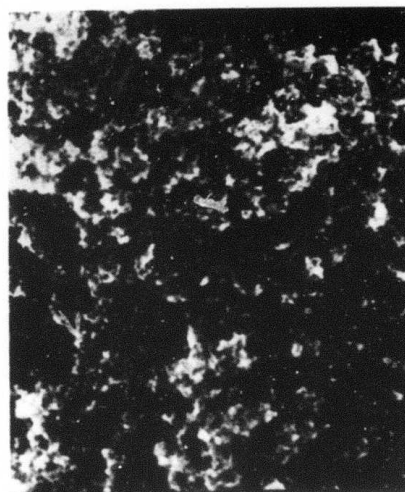
crystal growth observed is comparable to that seen in Figs. 2d or 3d. and certainly far more extensive than that observed with the film on the alumina substrate. In order to study chemical interactions without geometry effects sample type 5 was prepared in a manner identical to sample type 4 with the exception that pieces of the AlSiMag 614 substrate were added to the  $\text{RuO}_2$  and glass powder in the platinum crucible. Figure 6b. shows the microstructure obtained when sample type 5 was fired at  $1000^\circ\text{C}$  for 6 hours. This sintered mat with the absence of any appreciable crystal growth is identical to that of sample type 1, (Fig. 5b.), and clearly demonstrates that the inhibition of  $\text{RuO}_2$  crystal growth is the result of a chemical interaction with the substrate.

X-ray diffraction line broadening techniques were utilized to determine the crystallite sizes of sample types 1, 3, and 4. The 110 peak was scanned, using copper radiation at a speed of  $1/8$  degree/min in a Philips Norelco Diffractometer. The crystallite sizes were calculated from the Scherrer equation after the breadth at half the intensity was corrected for instrumental and  $K\alpha$ -doublet broadening according to the method outlined by Kaeble (13). The broadening caused by internal strains and other defects was neglected, but this is a fairly good assumption when ceramic powders are considered.

The average X-ray crystallite sizes for sample types 3 and 4 were found to be similar in agreement with the SEM studies (compare Figs. 2 and 3), but those for sample type 1 were much smaller, particularly at the higher temperatures. Data for sample types 1 and 4 as a function of time at temperature are shown in Fig. 7. The presence of the substrate appears to buffer the crystallite size after an initial rapid increase. This effect is



a. Sample 2



b. Sample 5

Figure 6. Effect of the Substrate on Growth of  $\text{RuO}_2$  Particles.  $1000^\circ\text{C}$ , 6 hours, 10,000 x.

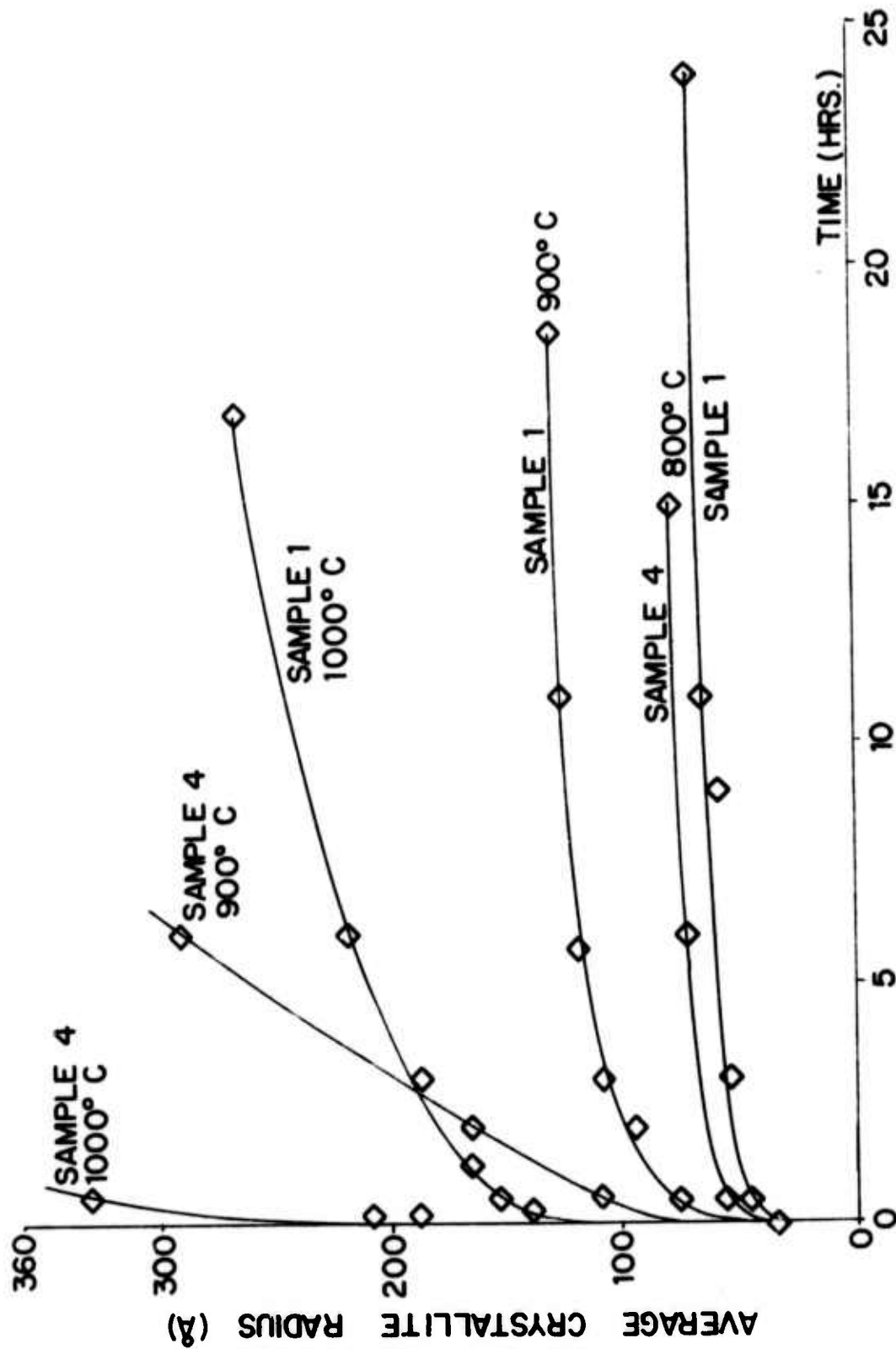


FIG. 7 AVERAGE CRYSTALLITE SIZE FROM X-RAY LINE BROADENING

probably due to a reaction between the substrate material and the glass, causing changes in the properties of the glass. These changes could result in either a decreased solubility of  $\text{RuO}_2$  in the glass or an increased viscosity of the glass, which would make diffusion of various species through it more difficult.

If one assumes that diffusion controlled solution-precipitation is the process for the particle growth in this system, then the average particle radius obeys the following time dependence (14).

$$[\bar{r}(t)]^3 - [\bar{r}(0)]^3 = \left( \frac{8\sigma_{SL} C_o D \Omega^2}{9RT} \right) t \quad (1)$$

$\bar{r}(t)$  = average particle radius at time  $t$ .

$\bar{r}(0)$  = average particle radius at time zero.

$C_o$  = equilibrium solubility at the temperature  $T$  ( $^{\circ}\text{K}$ ).

$D$  = diffusion coefficient.

$\Omega$  = molar volume.

$\sigma_{SL}$  = solid-liquid interfacial energy.

If the growth is reaction controlled then the following relationship holds (14):

$$[\bar{r}(t)]^2 - [\bar{r}(0)]^2 = \left( \frac{K_T C_o \sigma_{SL} \Omega^2}{RT} \right) t \quad (2)$$

where  $K_T$  is a transfer coefficient.

The above relationships can be applied to the X-ray diffraction line broadening data to find out whether the growth is reaction controlled or diffusion controlled.

In order to study the kinetics of ripening or sintering by solution-precipitation processes, one needs the particle size rather than the crystallite size. To this end, surface area measurements were carried out, using an Aminco Sor BET helium carrier surface area meter. The calculated BET surface area of the dried  $\text{RuO}_2$  powder used to fabricate all samples was  $70 \text{ m}^2/\text{gm}$ . which corresponds to an average particle size of about  $125\text{\AA}$ . The average X-ray crystallite size was calculated to be  $75\text{\AA}$ . A BET surface area measurement is expected to give a greater average particle size because of the clumping of the smaller particles, thus decreasing the surface area available for nitrogen absorption. Secondly, the packing factor of the powders has also to be considered. In the light of these considerations, it seems reasonable to assume that the X-ray crystallite size itself is the particle size. In addition, there is a good correlation between the particle size calculated from specific surface area and X-ray crystallite sizes of the samples after various firing temperatures and times as shown in Fig. 8.

Although good agreement is obtained between particles sizes of  $\text{RuO}_2$  (in the as dried condition) calculated from X-ray and from surface area measurements, the correlation with microstructure observations is not good. The SEM photographs previously reported (15) show the particle size of  $\text{RuO}_2$  in the dried powder to be within the range  $0.1$  to  $0.5 \mu\text{m}$ , but the average X-ray crystallite size is about  $75\text{\AA}$ . This order of magnitude difference is probably the result of agglomeration of the small  $\text{RuO}_2$  particles. Experiments conducted on compacts of  $\text{RuO}_2$  and glass showed that electrical continuity could be obtained on the as pressed samples ( $100,000 \text{ psi}$ ) even with  $10 \text{ w/o}$   $\text{RuO}_2$ , and on the pressed and fired samples ( $800^\circ\text{C} - 10 \text{ min}$ ) with even  $1 \text{ w/o}$   $\text{RuO}_2$ . If the theory of particle-to-particle contact were to hold good in these resistors, then it seems that this could only be possible if the

conductive particles are about  $75\text{\AA}$  as indicated by X-ray diffraction line broadening experiments. Because of the very small size and tendency to agglomerate, it is not possible to get a completely representative sample for SEM studies. Attempts to observe the  $\text{RuO}_2$  powder in the transmission electron microscope (TEM) did indicate a few particles in the range  $200\text{--}300\text{\AA}$ , but further experiments must be conducted to get a well separated sample for the TEM.

The results of the surface area measurements (Fig. 9) show a rapid decrease with time at  $1000^\circ\text{C}$  and a slow decrease at  $800^\circ\text{C}$ . This decrease is due to the network formation and/or the growth of bigger particles at the expense of the smaller ones. The surface area technique can be applied to study the initial stage sintering in the following way (16). Referring to Fig. 10, surface area at any time  $t$  for the two spherical particles undergoing sintering can be given

$$\begin{aligned} S_t &= 8\pi a^2 - 2\pi x^2 = S_o - K_1 x^2 \\ S_o - S_t &= K_1 x^2 \end{aligned} \quad (3)$$

If diffusion controlled solution-precipitation is the mechanism of sintering, then (17)

$$x^6 = K_2 t \quad (4)$$

where

$$K_2 = \frac{a^2 (24) (\delta) C_o \cdot \sigma_{LV} \Omega D}{RT}$$

and

$a$  = particle radius

$\delta$  = film thickness between the particles

$\sigma_{LV}$  = liquid vapor interfacial energy



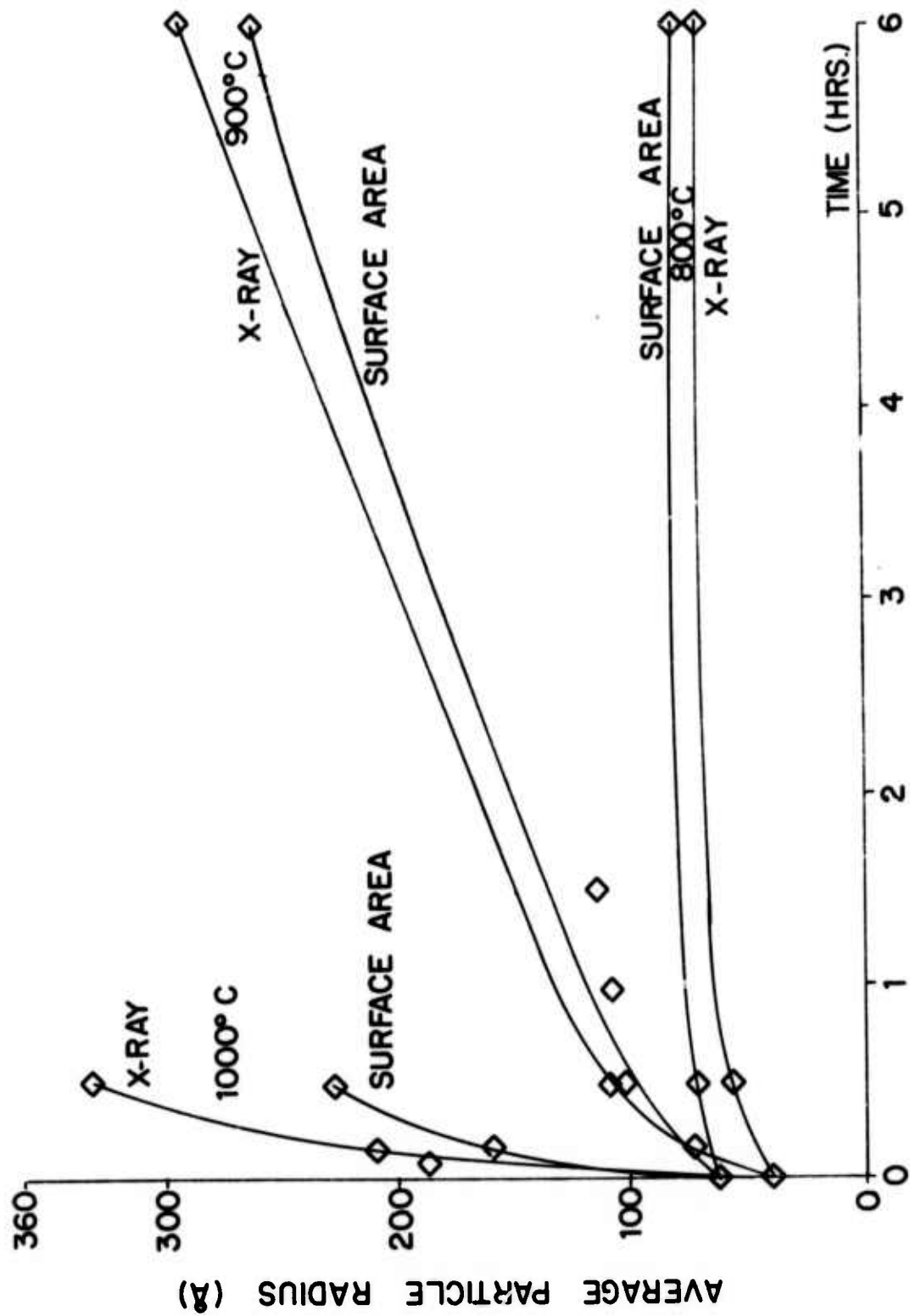


FIG. 8 PARTICLE SIZE OF SAMPLE 4 FROM X-RAY AND SURFACE AREA

From Eqs. (3) and (4)

$$(S_o - S_t)^3 = K_v t \quad \text{where} \quad K_v = K_1^3 K_2 \quad (5)$$

Hence, the slope of the straight line plots of  $(S_o - S_t)^3$  vs.  $t$  should give  $K_v$  which is related to the diffusion coefficient as,

$$\ln D = \ln K_v + \ln T - \ln (C_o \sigma_{LV}) - \ln (\text{constant})$$

Hence, from the plots of  $\ln K_v + \ln T - \ln (C_o \sigma_{LV})$  vs.  $1/T$  the activation energy for diffusion can be determined.

If phase boundary reaction leading to solution is the rate controlling step in the sintering process, then (17)

$$x^4 = K_3 t. \quad (6)$$

$$\text{where } K_3 = \frac{a^2 4 C_o^2 K \sigma_{LV} \Omega t}{RT}$$

$K$  = constant for the phase boundary reaction

From (3) and (6)

$$(S_o - S_t)^2 = K_u t \quad K_u = K_1^2 K_3.$$

In the previous report (18), the high temperature viscosity data for the molten lead-borosilicate glass was reported. If the Stokes-Einstein equation is assumed to be valid, then the diffusion coefficient follows the following relationship (19).

$$D = \frac{RT}{N} \cdot \frac{1}{3\pi\eta d}$$

$\eta$  = viscosity of the liquid

$d$  = diameter of the diffusing species

$N$  = Avogadro's number

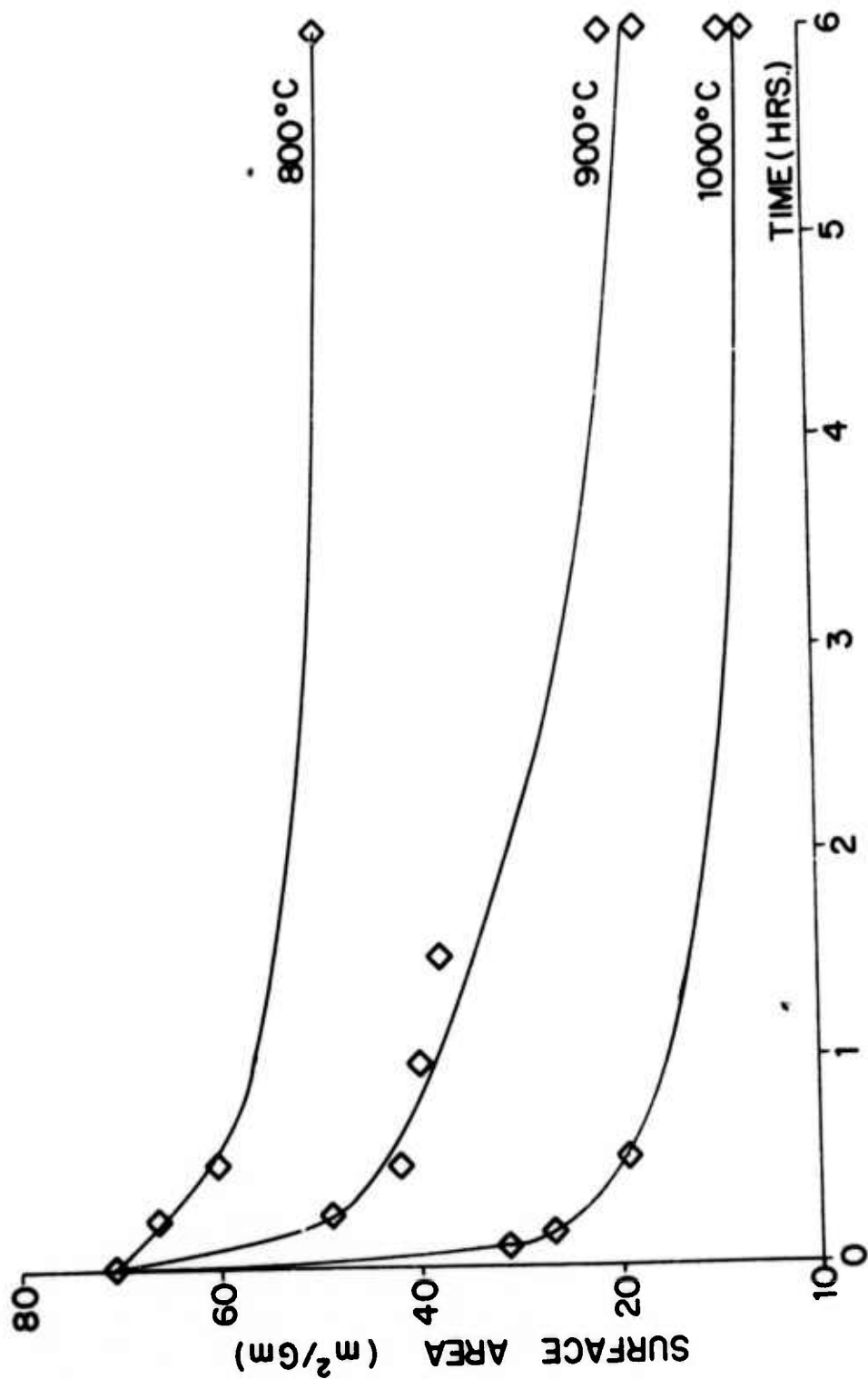


FIGURE 9 SURFACE AREA OF SAMPLE 4

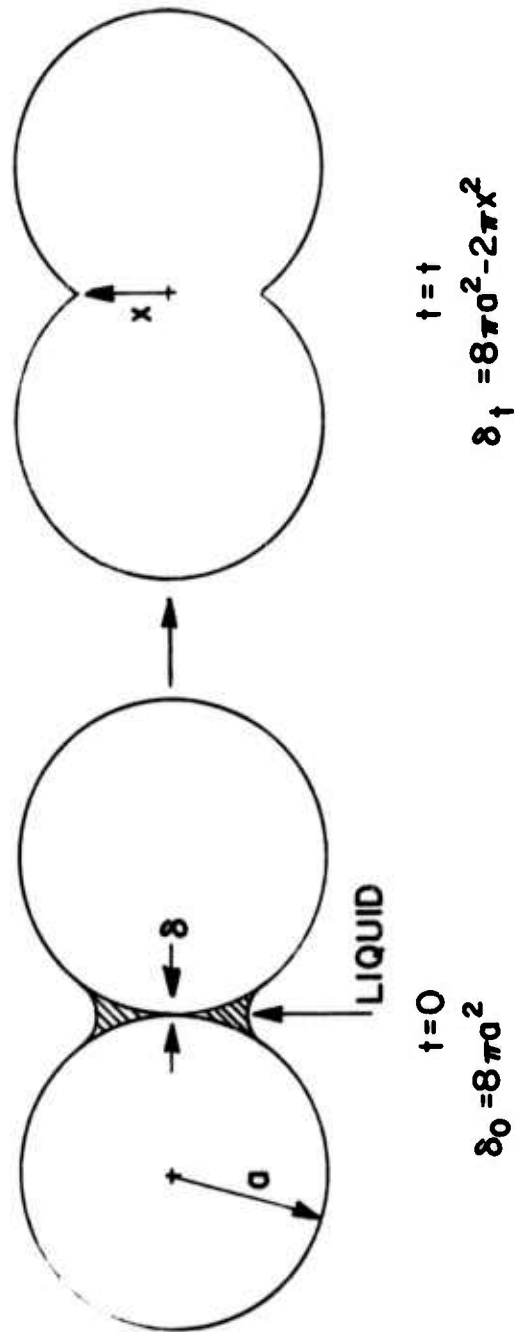
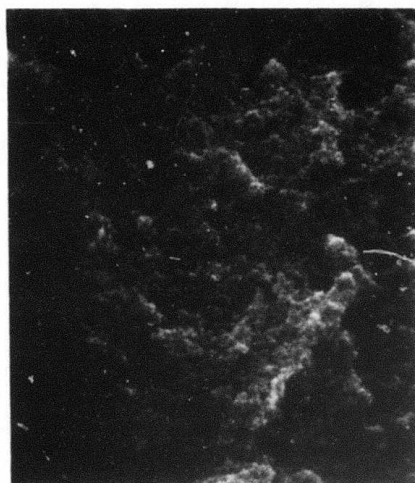


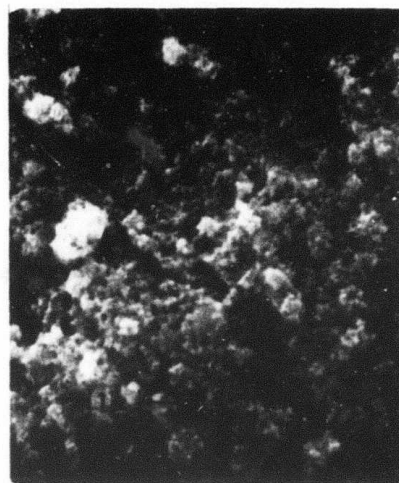
FIG. 10 LIQUID PHASE SINTERING GEOMETRY

Hence the activation energy calculated from these diffusion coefficients should correspond to the activation energy of viscosity.

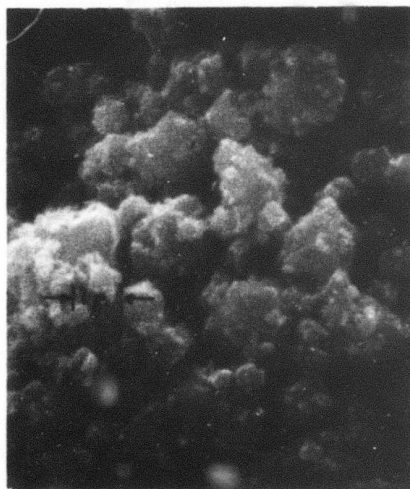
If the mechanism operating is diffusion controlled solution-precipitation, then parameters such as average X-ray crystallite size and surface area should be dependent on the proportions of glass and  $\text{RuO}_2$  in a random mixture. As the amount of glass is increased the diffusion length of the species increases and hence, at any temperature for certain time the average particle size and decrease in surface area should be smaller. Experiments were conducted using 18 w/o  $\text{RuO}_2$  in the powder mixture to determine the effect of the amount of the glass on the growth kinetics. These samples were fired at  $1000^\circ\text{C}$  for 10 minutes, 1/2 hour and 6 hours, and after removing all the glass checked for surface area, average X-ray particle size and the microstructure. The microstructure results are shown in Fig. 11. Results of the investigations were the same as those obtained for the samples containing 30 w/o  $\text{RuO}_2$  (compare Figs. 3 and 11) suggesting that the growth of  $\text{RuO}_2$  particles is independent of the amount of the glass. This would rule out the possibility that the growth process is controlled by diffusion limited solution-precipitation, except for the fact that the distribution of  $\text{RuO}_2$  in the glass is definitely not random. The same  $\text{RuO}_2$  microstructure, consisting of crystals growing on a sintered mat, is observed for both concentrations after equivalent time-temperature conditions indicating that the diffusion length is the same in both cases. An alternate experimental approach is required to establish the rate limiting step.



a. 10 minutes



b. 30 minutes



c. 6 hours

Figure 11. Sintering and Growth of  $\text{RuO}_2$  Particles - 18  $\omega/\text{o}$   $\text{RuO}_2$  plus Glass Powder Mixture Fired in a Platinum Crucible at  $1000^\circ\text{C}$  (10,000 x)

### III. SUMMARY AND FUTURE PLANS

#### A. Microstructure Development.

The sintering and ripening experiments described in this report will be continued until quantitative kinetic data are obtained and the various competing mechanisms sorted out. It was demonstrated that chemical interactions between the substrate and the glass have a dramatic effect on the ripening process of  $\text{RuO}_2$ . If the rate-limiting step in the sintering and ripening processes is the interface reaction leading to the dissolution at the small particles, (or diffusion through the glass after dissolution) then the way in which the addition of alumina or other substrate ingredients to the glass can alter this interface solubility (or transport rate) must be described. These are the remaining parameters needed to complete development of the phenomenological model for microstructure development.

#### B. Charge Transport Mechanisms.

Previously reported studies have shown that at least two types of charge transport processes are important in thick film resistors. A statistical model of a thick film resistor will be constructed which involves combinations of these mechanisms.

#### C. Test of Models.

The sheet resistance and TCR of resistors and conductors have been determined as a function of volume fraction of conductive phase to glass, and the results will be presented in the next semi-annual report. The important glass parameters, viscosity and surface tension, will be varied at constant thermal expansion and the results compared with predictions of the micro-

structure model and the interface model. Chemical additives which will alter the electrical properties according to the interface model but which will not affect microstructure development will be utilized to further test the interface model. Predictions of the microstructure and the interface model will be utilized to develop optimum resistor and conductor formulations within the given materials system. The performance of these will be evaluated according to the list of specifications developed previously.



#### IV. REFERENCES

1. R. W. Vest, Semi-Annual Technical Report for the period 7/1/70-12/31/70, Purdue Research Foundation Grant No. DAHC-15-70-G7, ARPA Order No. 1642, Feb. 1, 1971.
2. R. W. Vest, Semi-Annual Technical Report for the period 7/1/71-6/30/71, Purdue Research Foundation Grant No. DAHC-15-70-G7, ARPA Order No. 1642, August 1, 1971.
3. R. W. Vest, Semi-Annual Technical Report for the period 7/1/71-12/31/71, Purdue Research Foundation Grant No. DAHC-15-70-G7, ARPA Order No. 1642, Feb. 1, 1972.
4. R. W. Vest, Semi-Annual Technical Report for the period 1/1/72-6/30/72, Purdue Research Foundation Grant No. DAHC-15-70-G7, ARPA Order No. 1642, August 1, 1972.
5. R. W. Vest, Semi-Annual Technical Report for the period 7/1/72-12/31/72, Purdue Research Foundation Grant No. DAHC-15-70-G7, ARPA Order No. 1642, Feb. 1, 1973.
6. R. W. Vest, Semi-Annual Technical Report for the period 1/1/73-6/30/73, Purdue Research Foundation Grant No. DAHC-15-70-G7, ARPA Order No. 1642, August 1, 1973.
7. R. W. Vest, Semi-Annual Technical Report for the period 7/1/73-12/31/73, Purdue Research Foundation Grant No. DAHC-15-73-G8, ARPA Order No. 1001/192, February 1, 1974.
8. Page 3, Reference 3.
9. Page 10, Reference 6.
10. Page 4-5, Reference 6.
11. Page 45, Reference 5.

References (cont'd)

12. Page 19, Reference 3.
13. E. F. Kaedble, "Handbook of X-rays," McGraw-Hill, Inc., p. 17, 1-17, 8, 1967.
14. H. Fischmeister and G. Grimvall, MATERIALS SCIENCE RESEARCH 6, Ed. Kuczynski, Plenum Press, New York 1973, p. 119-149.
15. Page 46, Reference 5.
16. Wazo Komatsu, Yusuke Moriyoshi, Hidejiro Kawana, "Sintering of  $\text{RuO}_2$ ," Yogyo-kyokai-Shi, 80, 20 (1972).
17. W. D. Kingery, "Densification During Sintering in the Presence of a Liquid Phase. I. Theory," J. APPL. PHYS. 30, 301 (1959).
18. Page 6, Reference 7.
19. G. W. Greenwood, "The Growth of Dispersed Precipitates in Solutions," ACTA METALLURGICA, 4, 243 (1956).